

Article

Evaluation of Dynamic Properties of Trees Subjected to Induced Vibrations

Ernesto Grande ¹, Ersilia Giordano ²  and Francesco Clementi ^{2,*} 

¹ Department of Engineering Science, University Guglielmo Marconi, Via Plinio 44, 00193 Rome, Italy; e.grande@unimarconi.it

² Department of Civil and Building Engineering, and Architecture, Polytechnic University of Marche, Via Breccie Bianche, 60131 Ancona, Italy; e.giordano@pm.univpm.it

* Correspondence: francesco.clementi@staff.univpm.it

Abstract: The preservation of trees in urban and archeological areas is a theme of particular relevance. Modern systems of monitoring, together with approaches for deriving the main characteristics of trees influencing their response toward extreme events, are nowadays at the basis of a growing number of studies. The aim of the present paper is the dynamic identification of trees carried out by employing an approach which combines a simple data-acquisition system, direct and ambient sources of excitation, and different data-processing methods. In particular, using a single accelerometer placed at different sections of the trunk and considering excitations induced by either pulling tests or ambient vibrations, the derivation of the main frequencies and levels of modal damping characterizing the dynamic response of a sour cherry tree (*Prunus cerasus*) is carried out. A finite element model of the tree is also carried out to support the validation of the proposed approach and further analyze the derived outcomes. The obtained results underline the feasibility of the proposed approach in deriving information useful for assessing the behavior of trees toward dynamic actions and, consequently, of particular relevance for the identification of possible damages induced by variations in terms of dynamic characteristics (frequencies) and damping.

Keywords: dynamic identification; signal-data processing; power spectrum density; SDOF; FE model; least square fitting



Citation: Grande, E.; Giordano, E.; Clementi, F. Evaluation of Dynamic Properties of Trees Subjected to Induced Vibrations. *Appl. Sci.* **2023**, *13*, 7333. <https://doi.org/10.3390/app13127333>

Academic Editor: Giuseppe Lacidogna

Received: 26 May 2023
Revised: 14 June 2023
Accepted: 17 June 2023
Published: 20 June 2023



Copyright: © 2023 by the authors. Licensee MDPI, Basel, Switzerland. This article is an open access article distributed under the terms and conditions of the Creative Commons Attribution (CC BY) license (<https://creativecommons.org/licenses/by/4.0/>).

1. Introduction

Trees in urban areas are an important component of the landscape, contributing to improving the quality of life of the inhabitants. On the other hand, depending on their dimensions, architecture (size and configuration of trunk and branches), and position in the context of urban zones (streets, parks, squares, etc.), falling trees can also represent a dangerous situation for the safety of inhabitants, the integrity of surrounding structures, and the temporary interruption of common activities. At the same time, in the case of historical sites, ancient trees represent an integral part of the history of the site (a beautiful example is represented by the plane trees along the Tiber River in Rome), and the falling of these trees could affect the integrity of the cultural heritage of the site itself.

The attention of the scientific community toward the trees in urban areas is certainly testified by the relevant number of studies available in the literature ([1–7]) and also by the development of specific procedures based on both visual inspections and instrumental measurements. In particular, modern instruments were employed for monitoring the complex dynamic behavior of trees under wind actions [8], for measuring parameters specifically concerning the trees' geometry, and to investigate the internal structure of tree trunks [9].

In recent years, particular attention has also been devoted to the development of numerical models, similar to the ones employed for engineering structures, able to simulate the dynamic response of trees. Among these, of particular relevance are the models based on single- and multi-degree-of-freedom systems [10] and finite element models [11].

Both monitoring activity and numerical models are essential supports for performing the dynamic identification of trees [12].

Recent studies indeed focused the attention on the extension of dynamic identification approaches employed for engineering structures to trees. This certainly represents a possible important improvement to the current state of the art concerning the health monitoring and safeguarding of trees.

The use of the approaches developed for engineering structures (in particular building structures [13–18]) for studying the dynamic behavior of trees directly relies on the equivalence among the structural members (roots–foundations, trunk and branches–elevation structure, canopy–nonstructural elements) and their role within the structural system. Moreover, in terms of damage, a substantial similarity between trees and building structures can be observed. Indeed, damage influencing the structural response of buildings generally consists of defects due to the construction process, degradation of materials due to age or aggressive agents present in the environment, foundation movements due to phenomena at the level of the soil foundation, and local failures (cracks) induced by the occurrence of moderate/severe events during the life of a building. At the same time, in the case of trees, the process of growing could be affected by wood defects in both the trunk and branches, diseases or fungi leading to voids and wood degradation, variations in soil conditions leading to a loss of the anchoring function of roots with a consequent movement of the tree, and moderate/severe wind events inducing damage to the trunk or branches leading to changes in the level of vulnerability of trees toward the occurrence of subsequent wind events.

On the basis of this equivalence between trees and building structures, and taking into account the important differences between nature-made and man-made structures, the identification of dynamic properties of trees during their life (in particular before and after extreme events, or in the case where visual inspections underline specific signals on vegetation) could be of particular relevance for deriving information about damages affecting the safety level of trees toward future possible events.

From the analysis of past and recent literature, the use of different techniques (also employed in the present paper) for characterizing the dynamic response of trees emerges. Nevertheless, in the majority of cases, these techniques are used separately and, moreover, are carried out on the basis of data deduced from a relevant number of accelerometers (both along the trunk and branches [19]). The latter, in particular, makes them difficult to apply to practical applications involving a relevant number of trees to monitor.

In addition, the response of trees is generally assumed to be equivalent to that of an SDOF system, separately considering the behavior of the trunk and branches [10]. Then, the contribution of branches on the global response of trees in terms of modes of vibration and corresponding damping ratios is discarded. This aspect is instead considered by employing sophisticated finite element models for studying the dynamic behavior of trees [20].

2. Aims and Contents

This paper here presented is part of a research activity carried out by the authors within a multidisciplinary group of researchers for the development of health monitoring procedures for open-grown tall trees in urban and archeological areas based on dynamic identification.

The approach proposed in this paper is finalized to derive information on the dynamic behavior of trees in terms of vibration frequencies and modal damping ratios. To this end, in situ tests where a single accelerometer is placed on the trunk and simple data-analysis tools are employed to analyze the recorded signals are considered. Indeed, the approach combines the identification of frequencies of vibration carried out in the frequency domain on the basis of the recorded acceleration time histories, with the subsequent derivation of modal damping ratios derived by the superimposition of the dynamic response of N SDOF systems characterized by the identified frequency values. Regarding the latter, the authors also introduce the dependency of the frequency on the amplitude of motion to account for possible nonlinear effects characterizing the dynamics of trees. A schematic representation of the three main phases characterizing the proposed approach is shown in Figure 1, where

the preliminary phase concerning the in situ measurements carried out in terms of time history accelerations, the subsequent one concerning the identification of frequencies, and the third phase regarding the fitting of the response by superimposing the response of N SDOF systems are reported.

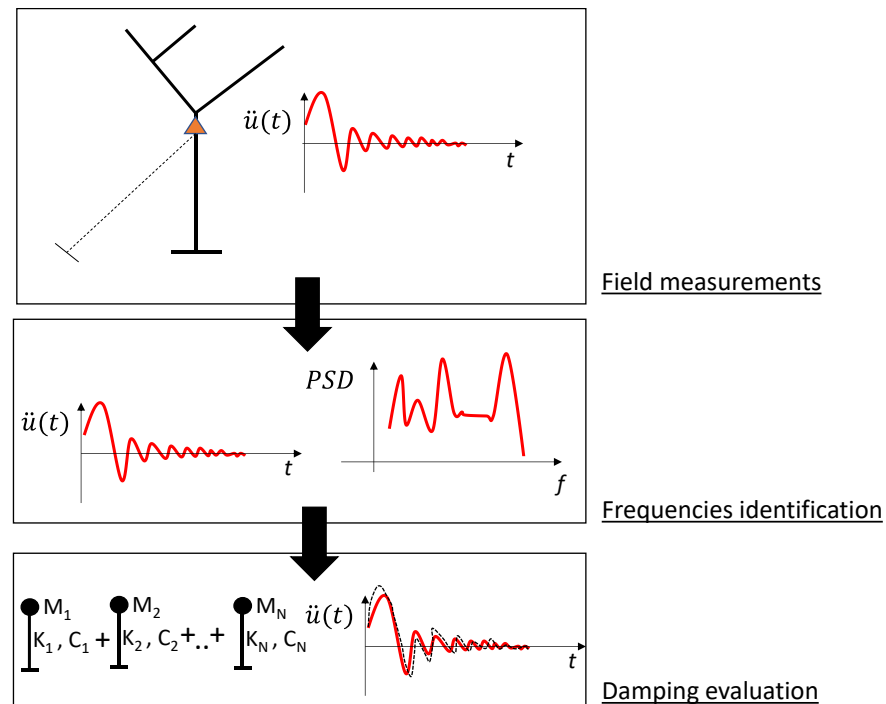


Figure 1. Flowchart of the main phases characterizing the proposed approach.

These features of the approach make it suitable for practical applications, particularly when a relevant number of trees are involved in the monitoring process. Indeed, besides the common information provided by static pulling tests or dynamic tests under wind conditions, which generally reduce to a safety factor, the approach allows for deriving additional parameters paramount for understanding the behavior of trees toward future dynamic actions and, in addition, for monitoring the health status of trees on the basis of variations in vibration frequencies and modal damping ratios—two important parameters related to the characteristics of trees.

The application of the proposed approach is carried out in this paper with reference to a sour cherry tree (*Prunus cerasus*) planted on a Roman archeological site in Italy. This case of study was selected in order to easily apply the proposed approach by considering a simple acquisition system together with different sources of excitation and, moreover, to carry out a finite element model of the tree for validating the results obtained from the approach.

The obtained results underline the feasibility of the proposed approach in deriving information useful for assessing the behavior of trees toward dynamic actions and, moreover, for the subsequent identification of possible damages induced by variations in terms of dynamic characteristics and damping.

3. Materials and Methods

3.1. Case Study and Site

The tree object of investigation is on a Roman archeological private site in Italy, and it is not protected by legal constraints. The site is inside the urban area, and it is characterized by an ellipsoidal shape with high ancient perimeter walls (from 4 to 10 m height) along north and west sides. Along the remaining parts of the perimeter, there is only a more recent perimeter wall (about 2 m height).

The tree case study, located on the east side about 10 m from the walls (Figure 2), is a young sour cherry tree (*Prunus cerasus*, about eight years old) with a simple architecture characterized by the trunk with a cross-section diameter at the base equal to 86 mm, and five main branches (Figures 2 and 3). Regarding the latter:

- A branch located next to the base of the trunk and mainly developing in the north–south (NS) vertical plane (this branch was subsequently cut);
- Two branches located at the same height (about 1.50 m from the base): one mainly developing in the NS vertical plane, the other one in a plane oriented at 25° from the NS vertical plane;
- Two branches at the upper extremity of the trunk (at about 2.50 m from the base): both mainly developing in the east–west (EO) vertical plane, one to the east and the other to the west.

During the field measurements presented in detail in the following, the tree did not present structural defects such as cavities, caries, etc., to both trunk and branches and it was without foliage. The latter aspect is of particular relevance in the context of this study because the application of the proposed approach is here aimed at obtaining information concerning the so-called internal damping [21] which is related to three main phenomena: interaction between roots and soil, structural damping due to the movement of branches, and the internal friction of wood. Indeed, this type of damping plays a relevant role toward the safety of trees in the case of strong winds occurring during the winter–autumn seasonal period. The presence of foliage, although, leads to an increase in the surface exposed to wind actions, also induces an increase in the level of damping (called external damping) mainly dependent on the aerodynamic drag of the crown.

The selection of a single (and simple) case study for the application of the proposed approach is dependent on the intention of developing a finite element model of the tree carried out on the basis of in situ and laboratory measures, to use as support tool for assessing and examining the data obtained from the proposed approach.



Figure 2. Overview of the site, the tree, and measurement setup (accelerometer). [Google Earth].

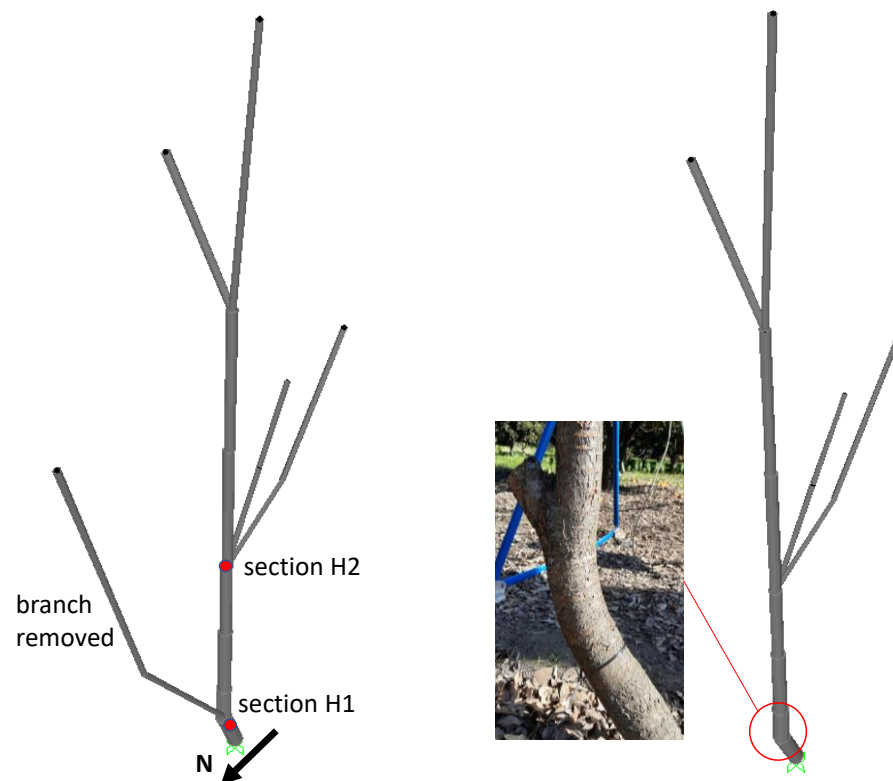


Figure 3. Schematization of the tree assumed as case study (trunk and main branches).

3.2. Field Measurements and Signal Elaboration

Field measurements were carried out by considering the excitations induced in the tree by pulling tests and ground vibrations due to agricultural machinery. Both tests were performed at the end of January 2023 under wind-free conditions and dry soil. The accelerations exhibited by the tree were recorded by means of a single accelerometer (acceleration range: ± 16 g; acceleration resolution: 0.005 g; sample frequency: 100 Hz) once placed at section H1 and once at section H2 of the trunk (Figures 1 and 2), along NS direction and EO direction. Sections H1 and H2 were selected in order to place the accelerometer near the removed branch (section H1) and near the two main branches.

Regarding the pulling tests, they were carried out by imposing a lateral displacement to the trunk of about 5 cm (either along NS direction or along EO direction) throughout a cord fixed at section H2, and then suddenly releasing it by inducing free vibrations to the whole tree. In addition, pulling tests were performed before and after removing the branch located near the base of the tree (Figure 3).

In detail, as reported in Table 1, four pulling tests were performed on the tree before removing the branch, and the same tests were performed after the removal of the branch located next to the base.

Regarding the field measurements in the case of ground vibrations, they concerned the accelerations induced to the tree (in this case the accelerometer was placed at section H2 only) by agricultural machinery (rotary tiller) working in proximity to the tree. In particular, the measurements were performed once along EO and once along NS directions (Table 1) when, in both cases, the agricultural machinery followed a squared path around the tree with a distance of about 2 m from the trunk.

As shown in Table 1, in order to identify the different tests, labels containing the indication of the removal of the branch (symbol 'r1'), the direction of the applied displacement (symbol 'T' followed by 'NS' or 'EO', respectively, for the directions north–south and east–west), and the direction of the recorded signal (symbol 'S' followed by 'NS' or 'EO',

respectively, for the directions north–south and east–west) were employed for pulling tests. In the case of ground vibration, the symbol ‘T’ was replaced by ‘GV’.

The results deduced from field measurements consisted of acceleration time histories recorded with a sample frequency of 100 Hz. In order to perform dynamic identification in the frequency domain of the main frequencies characterizing the dynamic response of the tree, the power spectrum density (PSD) function was evaluated for each measurement.

Table 1. Performed field measurements.

Pulling Tests				
Label	With/Without Branch (r1)	Pulling Section (H1/H2)	Pulling Direction (TNS/TEO)	Accelerometer Direction (SNS/SEO)
H1-TNS-SNS	with branch	section H1	north–south	north–south
H1-TEO-SEO	with branch	section H1	east–west	east–west
H2-TNS-SNS	with branch	section H2	north–south	north–south
H2-TEO-SEO	with branch	section H2	east–west	east–west
r1-H1-TNS-SNS	without branch	section H1	north–south	north–south
r1-H1-TEO-SEO	without branch	section H1	east–west	east–west
r1-H2-TNS-SNS	without branch	section H2	north–south	north–south
r1-H2-TEO-SEO	without branch	section H2	east–west	east–west
Ground Vibrations Tests				
Label	With/Without Branch (r1)	Accelerometer Direction (SNS/SEO)		
r1-GV-SNS	without branch	north–south		
r1-GV-SEO	without branch	east–west		

In particular, PSD was computed by using Welch’s method [22]. It consists of the following main steps:

- Partition of the data sequence X into a number K of segments (or batches), each composed of M number of points. The M -point sequence represents the window function. Among the commonly used window functions, they are the Rectangular, Harm or Hanning, Hamming, Blackman, Blackman–Harris, and Kaiser–Bessel. On the other hand, the parameter K represents the number of periodograms that are averaged together to form the PSD estimate;
- Computation for each segment of a windowed discrete Fourier transform (DFT) at some frequency values;
- Evaluation of the modified periodogram value from the discrete Fourier transform;
- Average of the periodogram values to obtain Welch’s estimate of the PSD.

This method is also called the Weighted Overlapped Segment Averaging (WOSA) method. Indeed, it requires the introduction of a parameter S referring to the number of points to shift between segments (it corresponds to the number of new points in each segment or batch). Consequently, two adjacent segments have $M-S$ points in common or, in other words, they are overlapped by $M-S$ points. This means that, in the case of $M = S$, the adjacent segments do not overlap. Whilst, in the case of $S = 0.5 M$, adjacent segments contain 50% overlap [22].

In this paper, the PSD estimate was carried out by using the function `pwelch` available in Matlab [23].

3.3. Numerical Models

In order to analyze the results deduced from the dynamic identifications, two simplified models were employed.

The first one consisted of approximating the dynamic response of the tree due to free vibrations induced by pulling tests throughout the dynamics of a single-degree-of-freedom (SDOF) viscously damped system subjected to free vibrations.

Then, starting from the equation of motion governing the free vibration of SDOF,

$$m\ddot{u} + c\dot{u} + ku = 0 \tag{1}$$

where m is the lumped mass of SDOF; c is the damping constant, representing a measure of the energy dissipated in a cycle of free vibration; k is the stiffness of SDOF; u , \dot{u} , \ddot{u} are the displacement, velocity, and acceleration functions of the time t , respectively, introducing the initial conditions in terms of displacement and velocity characterizing the pulling test:

$$\begin{aligned} u(0) &= u_0 \\ \dot{u}(0) &= 0 \end{aligned} \tag{2}$$

and considering the case of underdamped systems ($c < 2\sqrt{k \cdot m}$), the solution of Equation (1) in terms of displacement can be obtained:

$$u(t) = \rho \cdot \cos(\omega_D t + \theta) \exp(-\zeta \omega_n t) \tag{3}$$

where:

$$\begin{aligned} \zeta &= \frac{c}{2\sqrt{km}}: \text{equivalent damping ratio;} \\ \omega_n &= \sqrt{\frac{k}{m}}: \text{natural circular frequency;} \\ \omega_D &= \omega_n \sqrt{1 - \zeta^2}: \text{damped circular frequency.} \end{aligned}$$

ρ and θ are, respectively, the amplitude of motion and the phase angle that, considering the initial conditions of Equation (2), in particular, the initial velocity equal to zero, result in the following:

$$\rho = \sqrt{u(0)^2 + \left(\frac{\dot{u}(0) + u(0)\zeta\omega_n}{\omega_D}\right)^2} = \sqrt{u(0)^2 + \left(\frac{u(0)\zeta\omega_n}{\omega_D}\right)^2} \tag{4}$$

$$\theta = -\tan^{-1}\left(\frac{\dot{u}(0) + u(0)\zeta\omega_n}{u(0)\omega_D}\right) = -\tan^{-1}\left(\frac{\zeta\omega_n}{\omega_D}\right) \tag{5}$$

Consequently, the corresponding solution in terms of acceleration can also be obtained:

$$\ddot{u}(t) = \rho \cdot \left[\cos(\omega_D t + \theta) (\zeta^2 \omega_n^2 - \omega_D^2) + 2 \sin(\omega_D t + \theta) \zeta \omega_D \omega_n \right] \exp(-\zeta \omega_n t) \tag{6}$$

The obtained solution describes the free-vibration response of SDOF in terms of accelerations. Then, in case the response in terms of acceleration is experimentally available and, moreover, frequency is deduced from a dynamic identification process, the above equation could be directly used for estimating the level of damping.

This approach is presented in this paper where the measured response of the tree in terms of acceleration (time history provided by the accelerometer) has been fitted by the numerical response of an SDOF system considering the values of the identified frequencies and opportunely setting the level of damping ratio. This approach resulted in being particularly useful in providing qualitative information about the influence of the architecture of the tree on both the dynamic response and, moreover, the level of modal damping. Indeed, the accelerations measured at the level of the trunk are influenced by the dynamics and the contribution in terms of damping of both the trunk and branches (and roots).

At the same time, in order to improve the level of approximation of the experimental response obtained by the above approach, according to the method proposed in [24], a least square fitting considering the superimposition of the response of N SDOF systems was also carried out:

$$\ddot{u}(t) = \sum_{i=1}^N \rho_i \cdot \left[\cos(\omega_{D,i}t + \theta_i) \left(\xi_i^2 \omega_{n,i}^2 - \omega_{D,i}^2 \right) + 2 \sin(\omega_{D,i}t + \theta_i) \xi_i \omega_{D,i} \omega_{n,i} \right] \exp(-\xi_i \omega_{n,i} t) \tag{7}$$

In particular, to account for nonlinear effects, the natural frequency was introduced in the minimization process in the following form:

$$\omega_{n,i} = \omega_{0,i} + k_{1,i} \cdot \rho_i^2 \tag{8}$$

where $\omega_{0,i}$ is the linear circular natural frequency of the i -th SDOF, ρ_i is the amplitude of motion, and $k_{1,i}$ is the corresponding nonlinear correction coefficient [21]. As shown in the following, the choice of the number N of SDOFs to combine was selected on the basis of the results emerging from PSD functions.

For both the above approaches, the minimization process was performed by measuring the quality of the approximation through the following dimensionless index [21]:

$$I_1 = \frac{\sqrt{\frac{\sum_{j=1}^n (\ddot{u}_j - \ddot{u}_j^*)^2}{n}}}{\max_t \{ \ddot{u}_j^*(t) \}} \tag{9}$$

where

- n is the number of time steps composing the recorded signals;
- \ddot{u}_j is the acceleration at the time j deduced from the least square fitting;
- \ddot{u}_j^* is the acceleration at the time j deduced from the experimental measurements.

The second model employed in this paper for the analysis of the dynamic behavior of tree consisted of a finite element model where both trunk and main branches were modeled as Eulero–Bernoulli beam elements. This model represents a supplement to the study. Indeed, it was used to understand some features of vibration modes of the examined tree and, then, for better figuring out the results deduced from the proposed approach. In order to provide a good approximation of the dynamic response of the tree considering the trunk and main branches only, the following parameters were considered:

- For the trunk and branches, the mean value of the corresponding measured diameters was assigned to beam elements (then characterized by a constant section along their length);
- Regarding the material, an isotropic material was considered for both trunk and branches by introducing the following parameters:
- Self-weight $\gamma = 1010 \text{ kg/m}^3$, directly deduced by measuring in laboratory the weight and volume of specimens obtained from the removed branch. This value was increased by 50% in the FE model for branches only in order to account for the weight of secondary branches not included in the FE model;
- Young’s modulus $E = 4 \text{ GPa}$, experimentally evaluated by performing simple cantilever tests on two specimens deduced from the removed branch: $E = \frac{F \cdot L^3}{3 \Delta I}$, where F and Δ are, respectively, the load applied at the free end of specimen and the corresponding measured displacement; L is the length of the specimen; I is the cross-section moment of inertia evaluated by approximating the effective section of specimens as circular and considering an average value of diameter;
- At the base of the model (i.e., the base of the trunk), a rotational spring was inserted around both X and Y axes (respectively, corresponding with EO and NS directions). A rotational stiffness value $K_\phi = 13 \text{ kNm/rad}$ was calculated by simply measuring the rotation at the base of the tree during the pulling test. This component was introduced in the FE model to simulate the movement of the tree at the level of roots, which could particularly affect the dynamic properties of tree [19].

The obtained FE model was particularly useful to derive considerations about the modal shapes corresponding to the identified frequencies.

4. Pulling Test Field Measurements Results

The results deduced from the pulling tests in terms of the recorded accelerations, before and after the removal of one of the main branches, were analyzed to identify the main frequency values characterizing the dynamic response of the tree subjected to induced free vibrations. The analyses were performed by considering the dynamic response of the tree subjected to free vibrations along the two accounted directions (EO and NS) and considering the recordings at the base of the trunk (section H1) and at section H2.

The results are graphically presented in Figures 4 and 5 in terms of the PSD function reported in the logarithmic scale in order to better point out the identified frequencies.

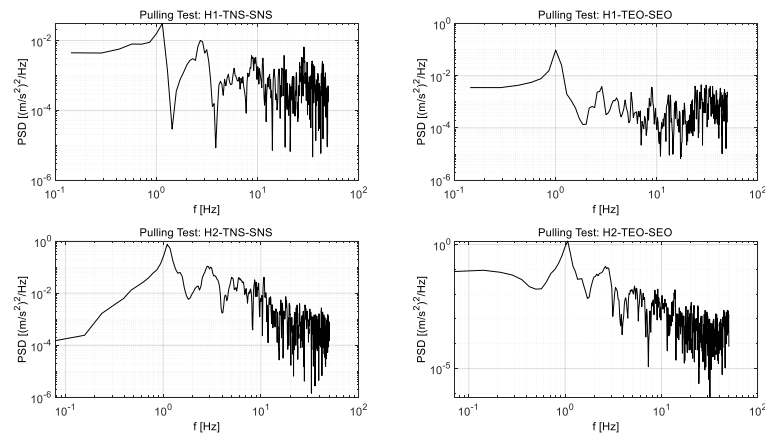


Figure 4. PSDs of signals deduced from pulling tests before removing the branch.

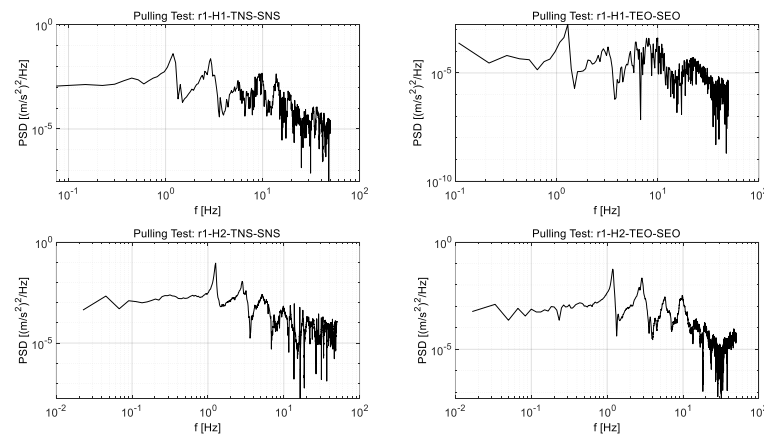


Figure 5. PSDs of signals deduced from pulling tests after removing the branch.

Considering the main peaks that emerged from the PSD functions in the range 0–10 Hz, it is possible to observe the following:

- The greatest peak of the PSD functions for all the performed tests corresponded to the lowest identified frequency value (about 1 Hz);
- The second peak corresponded to a range of frequencies varying between 2.5 and 3.0 Hz (except in the case of the tests H1-TEO-SEO and r1-H1-TEO-SEO where this peak was not evident);
- The subsequent main peaks identified two other frequencies with values approaching about 5 Hz and 10 Hz, respectively;
- The comparison between the values of the frequency identified before and after the removal of the branch underlined for the majority of cases a slight increase in frequencies (i.e., a reduction in periods of vibration) probably mainly due to the reduction in mass (it was estimated that the mass of the removed branch was about

- 1/3 of the mass of the tree). This outcome emphasized that for the accounted case, the removal of the selected branch did not induce a significant variation in the dynamic response of the tree;
- The arrangement of the accelerometer at section H2 allowed for better identifying the frequencies from the PSD functions with respect to section H1: at the base of the tree a curvature of the trunk with a local increase in the section due to the presence of the removed branch was indeed present (Figure 3).

5. Ground Vibration Field Measurements Results

A second set of results was carried out from the measurements obtained in the case of the ground vibrations induced by typical agricultural machinery working in proximity to the tree (Figure 6).

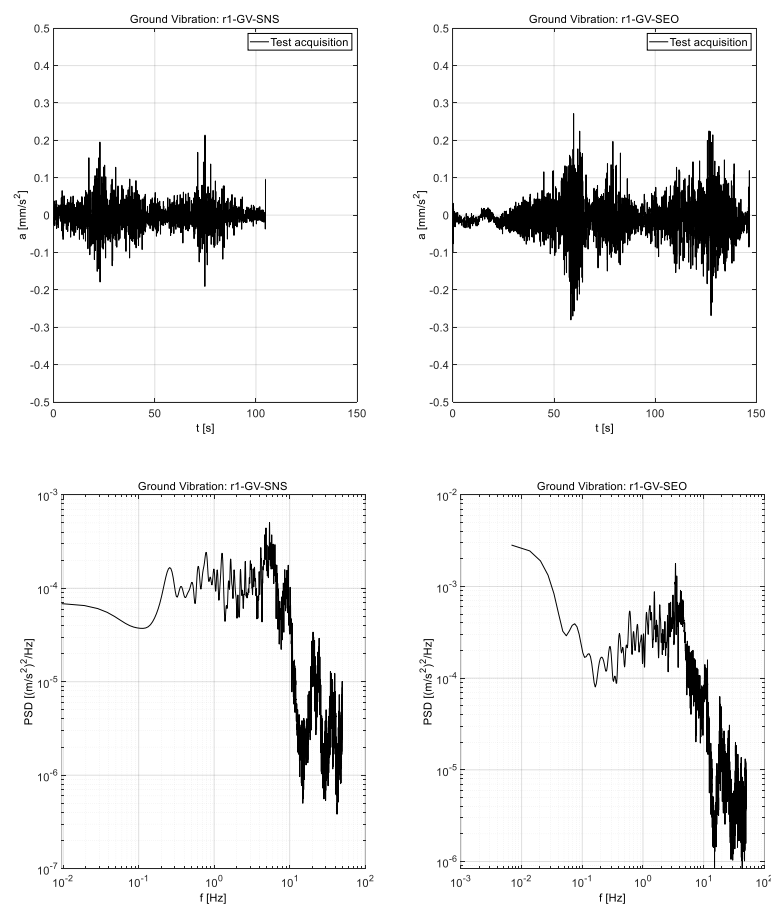


Figure 6. Registered accelerations (**top**) and PSDs (**bottom**) deduced from ground vibration tests (the derivation of PSDs is carried out by using a rectangular window of length $L/8$, where L is the length of signal).

In particular, because the available setup only consisted of one accelerometer, the two measurements were performed separately but considered the same path of the agricultural machinery: a squared path around the tree with a distance of about 2 m from the trunk. Although the two recorded signals showed differences mainly due to the alteration of the status of the soil after the first transit of the agricultural machinery, similar peaks of accelerations were induced to the trunk (Figure 6).

In this case, different from the pulling tests, the accelerations were measured in section H2, and in the case of the removal of the branch only, still along the EO and NS directions. The recorded accelerations normal to the axis of the trunk in this case were induced by

the horizontal and vertical vibrations of the ground instead of an imposed displacement normal to the axis of the trunk.

Like the approach presented for the pulling tests, the dynamic identification was still performed by deriving PSDs from the recorded signals (see Figure 6). In this case, it was observed that, considering a window length equal to the length L of the signal, a not clear identification of the main frequencies characterizing the dynamic response of the tree emerged from the PSDs (probably due to the presence of forced vibrations). To provide better identification, the length of the time window was reduced by assuming a length value equal to $L/8$ and, consequently, increasing the number of segments and considering 50% overlap. This adoption allowed to improve the identification of frequencies.

Although the differences emerged from the analysis of the two signals (i.e., along the two accounted directions), the obtained results underlined peaks in a range of frequencies between 0 and 5 Hz and around 10 Hz.

Comparing the PSD functions, the predominance of the vibration mode characterized by a frequency approaching 5 Hz emerged (i.e., the third mode identified in the case of pulling tests). Two other modes still emerged from the PSD functions: the first mode (the one characterized by a frequency approaching 1 Hz) and the fourth mode (characterized by a frequency approaching 10 Hz). The second mode was slightly evident only for the measurement along the NS direction.

Although the case of the ground vibrations led to a condition of forced vibrations for the tree, which is different from the case of free vibrations induced by the pulling tests, the result deduced from the identification in the frequency domain underlined peaks of the PSD corresponding to the natural frequencies deduced from the pulling tests. The greater number of peaks was due to both different excited modes in the case of ground vibrations and, at the same time, forcing vibrations. The vibration modes (and then the corresponding frequencies) identified from the ground vibrations provided a validation of the data deduced from the pulling tests and, at the same time, they showed a dynamic response to ground vibrations particularly involving the higher modes (i.e., those generally influenced by the dynamics of branches). Indeed, different from the PSDs deduced from the pulling tests, here the peaks corresponding to frequencies in the range 20–25 Hz and 35–40 Hz were clearly recognizable.

6. Considerations

The results carried out from the pulling tests emphasized the dynamic behavior of the tree along both directions, influenced by both lower and higher modes of vibration. This is typical behavior of decurrent trees where the main branches could play an important role in the dynamic response.

In order to analyze this aspect for the accounted case of study, the PSD functions of the signals recorded from the accelerometer were carried out by dividing the signal into two subsequent time windows: the first one from 0 to 8 s and the second one from 8 to 60 s. In Figure 7, the whole recorded signal is reported in the case of the pulling tests r1-H2-TEO-SEO together with the two accounted segments, one for each of the two time windows.

From the figure, it is quite evident that, while the signal in the first time window was particularly influenced by higher modes (the shape of the signal deviated from the one of a simple harmonic), this effect was less evident in the subsequent time sequence. Indeed, deriving the PSD functions separately for the two accounted time windows (the PSD was normalized with respect to the total energy E_{tot} of the corresponding signals), it is possible to observe the following (Figure 8): while from the PSD corresponding to the first time window the frequencies related to both the lower and upper modes of vibration clearly emerged, from the PSD of the subsequent time window mainly emerged the frequency corresponding to the lowest identified mode.

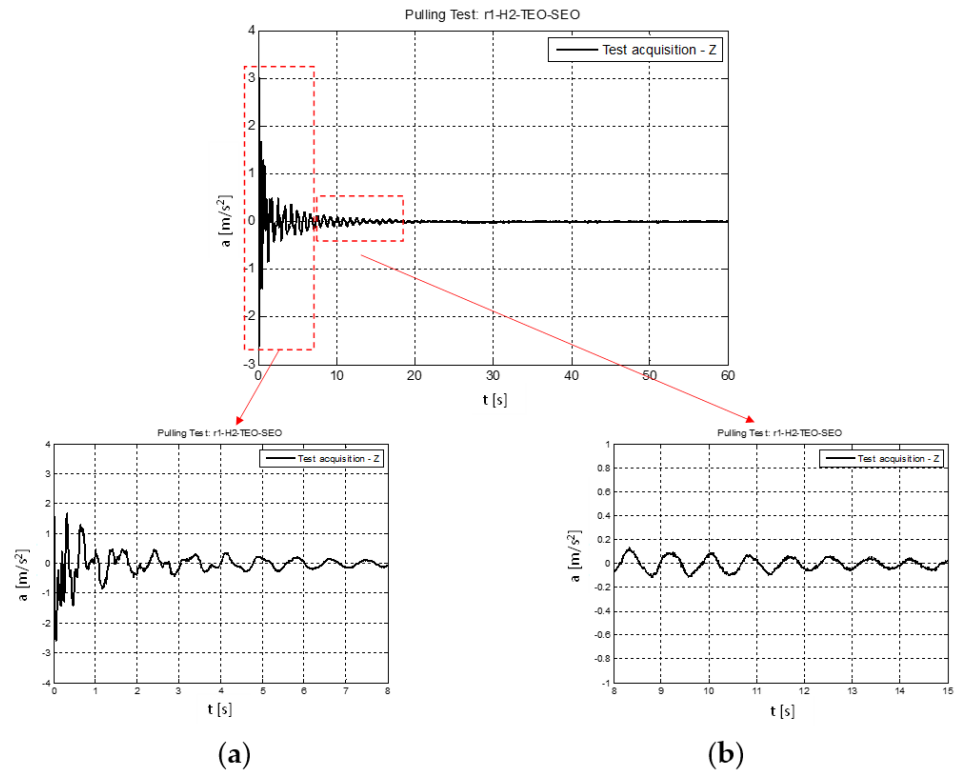


Figure 7. Signal recorded from pulling test: (a) zoom of signal on the first accounted time window; (b) zoom of signal on a portion of the second time window.

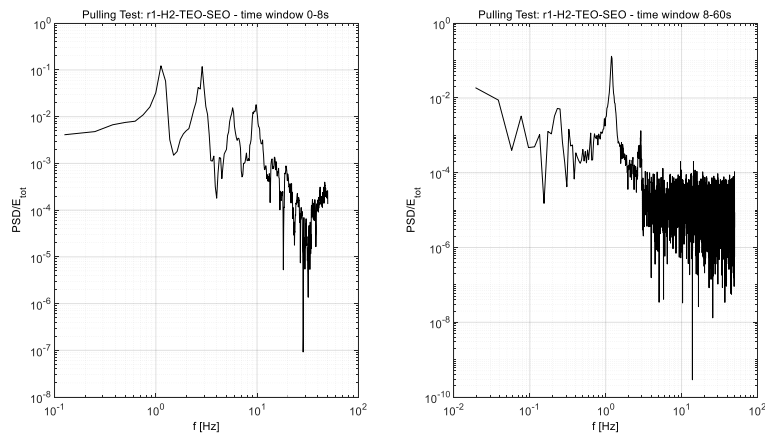


Figure 8. PSDs deduced from pulling tests performed after removing the branch for the two selected time windows: (left), time window from 0 to 8 s; (right), time window from 8 to 60 s.

This outcome is of particular relevance. Indeed, analyzing the results deduced in terms of the mode shapes from the FE model here carried out (Figure 9), it clearly emerged that the first two modes (characterized by similar values of frequency, about 1.6 Hz, and mainly translational along the two directions EO and NS, respectively) were mainly related to dynamics involving the whole tree (Figure 8). Differently, the upper modes were particularly influenced by the dynamics of branches with a lower participating mass ratio (Figure 9).

The trunk and branches were responsible for the damping of the tree—a further complex parameter influencing the dynamic response toward the different actions.

Then, in order to carry out considerations concerning this additional parameter, although the dynamic response of the tree to free vibrations underlined a behavior typical of MDOF systems, the recorded acceleration time histories were approximated by the

response of an SDOF viscously damped system, by opportunely varying the value of the equivalent damping ratio (Figure 10). In particular, it was considered that the first time window was from 0 to 8 seconds, while the second time window accounted for a reduced duration, from 8 s to 15 s, to reduce the effect of the noise characterizing the subsequent time.

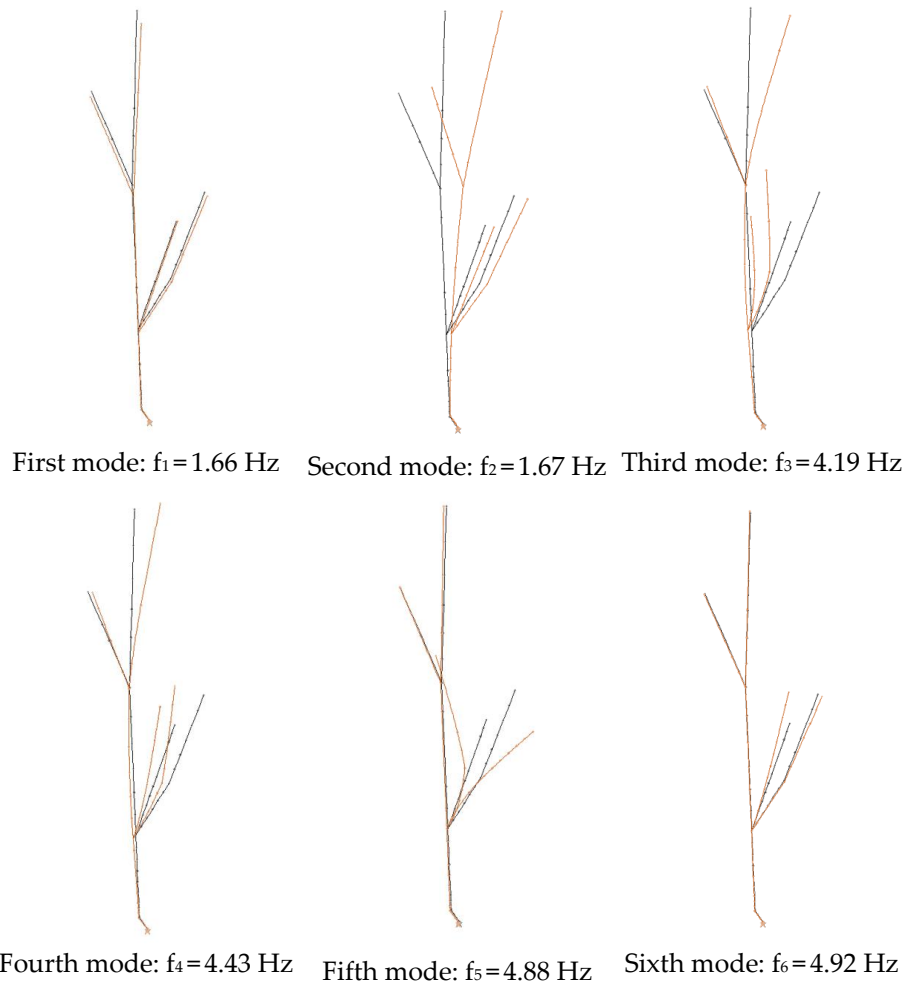


Figure 9. Modal shapes deduced from the FE model (deformed shape in orange).

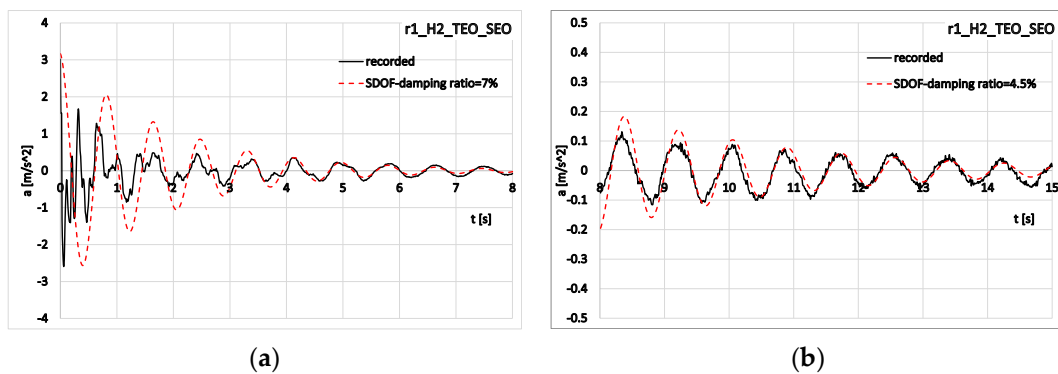


Figure 10. Approximation of the recorded signal by the response of the SDOF system: (a) first time window, 0–8 s— $I_1 = 0.26$; (b) second time window, 8–15 s— $I_1 = 0.19$.

The obtained results underlined, as expected, a greater value of the damping ratio for the first time window (i.e., the one influenced by the higher modes), whilst a significantly lower value of the damping ratio characterized the second part, i.e., the part of the response

of the trunk not significantly influenced by the dynamics of the branches. In particular, from Figure 10a, a greater level of damping emerged with respect to the theoretical one deduced from the numerical model. This outcome underlined both the influence of the upper modes and, at the same time, the complexity of the phenomenon (particularly when the dynamic of branches is involved), and then the level of approximation in considering a simple model of viscous damping.

The same approach carried out for the tree before removing the branch underlined a similar behavior and, also, similar values of damping ratios. Consequently, it also emerged that the removed branch did not provide a significant contribution to the damping of the tree, probably mainly due to its position at the base of the tree.

Finally, the least square fitting was carried out on the whole length of the signal by superimposing the response of $N = 4$ SDOF systems (the number N of SDOFs was selected on the basis of the number of the main peaks emerging from the PSD functions). The obtained results are graphically presented in Figure 11 by comparing the recorded response and the one obtained from the least square fitting. From the figure, the role played by the combination of the SDOF responses particularly in the first eight seconds was evident. Indeed, comparing the ‘quality’ of the least square fitting with the one characterizing the fitting made by considering an SDOF behavior, the lowest value of the index I_1 in the case of the least square fitting was evident.

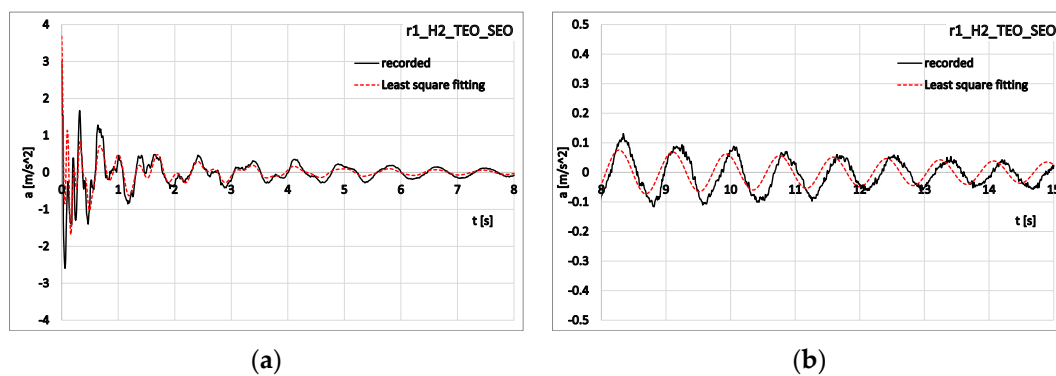


Figure 11. Least square fitting of the whole recorded signal: (a) zoom of results on 0–8 s; (b) zoom of results on 8–60 s.

Moreover, by examining the results reported in Table 2, also in this case, the greater level of damping associated to the upper frequencies emerged. Considering the values of the amplitude of motion ρ_i , it could also be observed that the first two modes particularly contribute to the global response, whilst the third one was the least important.

Table 2. Results deduced from the numerical approximation for the recorded response (r1_H2_TESO_SEO).

Time Window	N	ρ_i (m)	ζ_i	$\omega_{0,i}$ (rad/s)	$k_{1,i}$	I_1
0–60 s	1	0.0034	0.0153	7.59	0.5202	0.0314
	2	0.0027	0.0480	18.50	0.7995	
	3	0.0004	0.1578	33.94	0.7072	
	4	0.0008	0.1160	57.62	0.1347	
0–8 s	1	0.055	0.070	7.58	-	0.2587
8–15 s	1	0.055	0.045	7.50	-	0.2129

7. Conclusions

Health monitoring of trees in urban and archeological areas is a topic of particular interest involving the specialist and diversified skills of professional figures.

The dynamic of trees is particularly complex because it is strictly related to its intricate architecture (i.e., configuration of trunk and branches) and the variability in the characteristics of wood material. Both these properties, moreover, change over time. Accelerations induced through pull–release tests or ambient excitations are strictly influenced by the characteristics of trees. The advances in the field of forest sciences together with modern instruments and approaches, some of which are carried out in engineering fields, allow for identifying important parameters, such as the frequency of vibrations and damping ratio, useful for studying the dynamic response of trees toward actions often responsible for their falling.

In this paper, the dynamic identification of a tree case study has been presented by proposing an approach which combines a simple data-acquisition system, different sources of excitation, and elaboration approaches based on both common signal processing in the frequency domain and simplified numerical models.

The following main outcomes have emerged from the study:

- The results deduced from the approach have allowed to derive features characterizing the dynamic response of the tree toward the accounted sources of excitation by combining among them the adopted tools.
- The use of the power spectrum density has underlined the main frequencies governing the dynamic response of the tree, before and after removing one of the main branches and considering different positions of the accelerometer along the trunk. In particular, clearer identification in the case of the accelerometer located distant from the base of the trunk has been observed. Moreover, it has been observed that the removal of the branch placed near the base of the trunk did not induce significant variations in the frequencies.
- The schematization carried out by using the SDOF model and finite element model has allowed for deriving additional information concerning the level of damping and modal shapes, strictly correlated among them and playing a key role toward other types of excitations, such as wind actions. In particular, it has been observed that, while the lower modes involved a dynamic of the whole tree with a low value of the damping, the upper modes mainly involved the dynamic of branches that particularly increased the damping of the tree.
- The results obtained from the least square fitting pointed out levels of the modal damping ratio equal to 1.5% and 5%, respectively, for the first and second mode of vibration (in agreement with the values experimentally found and suggested by different authors [12,21]) and equal to 12% and 16% for the third and fourth mode, respectively. The high values of the latter are probably influenced by the nonlinear nature of damping, its dependency on the amplitude of motion, and the approximation in using a pure viscous model [12].

8. Future Developments

Regarding future possible developments, in agreement with the more general goal of the research activity carried out by the authors, further measurements and elaborations using the same approach, improved by considering a nonlinear model for damping, will be carried out to assess the variation in frequencies of vibration and damping due to seasonal variations in trees and, also, variations in soil conditions. This will be of particular relevance to account for the specific features of the living nature of trees with respect to man-made structures, and their influence on the effectiveness of the dynamic identification process.

Additionally, because one of the main goals of the research activity is the prediction of the behavior of trees toward possible severe actions, taking into account the occurrence of damage states, a further topic to investigate necessarily will concern the mechanism of damage in trees. To this end, still considering the equivalence between trees and buildings, an interesting basis could be represented by the studies available in the literature concerning the mechanism of damage in geomaterials. For instance, in [25], a study was conducted concerning the influence of shear stress concentrations on damage and failure processes by proposing specific analytical models that can be opportunely applied to trees.

Finally, because the proposed approach allows for a fast identification of trees' dynamic properties, it could benefit from the data deduced on a large scale (for instance, from satellite imagery approaches [26,27]). At the same time, it could support the prediction of large-scale failure scenarios by using the identified data on tree samples just selected on the basis of satellite survey.

Author Contributions: Conceptualization, E.G. (Ernesto Grande), E.G. (Ersilia Giordano) and F.C.; methodology, E.G. (Ernesto Grande), E.G. (Ersilia Giordano) and F.C.; formal analysis, E.G. (Ernesto Grande), E.G. (Ersilia Giordano) and F.C.; field measurements, E.G. (Ernesto Grande); writing—original draft preparation, E.G. (Ernesto Grande), E.G. (Ersilia Giordano) and F.C.; writing—review and editing, E.G. (Ernesto Grande), E.G. (Ersilia Giordano) and F.C.; visualization, E.G. (Ernesto Grande), E.G. (Ersilia Giordano) and F.C.; supervision, E.G. (Ernesto Grande) and F.C. All authors have read and agreed to the published version of the manuscript.

Funding: This research received no external funding.

Institutional Review Board Statement: Not applicable.

Informed Consent Statement: Informed consent was obtained from all subjects involved in the study.

Data Availability Statement: No new data were created.

Conflicts of Interest: The authors declare no conflict of interest.

References

- Lüttge, U.; Buckeridge, M. Trees: Structure and function and the challenges of urbanization. *Trees* **2020**, *37*, 9–16. [\[CrossRef\]](#)
- Locosselli, G.M.; Buckeridge, M.S. The science of urban trees to promote well-being. *Trees* **2023**, *37*, 1–7. [\[CrossRef\]](#)
- Pretzsch, H.; Moser-Reischl, A.; Rahman, M.A.; Pauleit, S.; Rötzer, T. Towards sustainable management of the stock and ecosystem services of urban trees. From theory to model and application. *Trees* **2021**, *37*, 177–196. [\[CrossRef\]](#)
- Gonçalves, R.; Linhares, C.; Yojo, T. Drag coefficient in urban trees. *Trees* **2020**, *37*, 133–145. [\[CrossRef\]](#)
- Ow, L.F.; Harnas, F.R.; Indrawan, I.G.B.; Sahadewa, A.; Sim, E.K.; Rahardjo, H.; Leong, E.C.; Fong, Y.K.; Tan, P.Y. Tree-pulling experiment: An analysis into the mechanical stability of rain trees. *Trees* **2010**, *24*, 1007–1015. [\[CrossRef\]](#)
- Reubens, B.; Poesen, J.; Danjon, F.; Geudens, G.; Muys, B. The role of fine and coarse roots in shallow slope stability and soil erosion control with a focus on root system architecture: A review. *Trees* **2007**, *21*, 385–402. [\[CrossRef\]](#)
- Abbas, S.; Kwok, C.Y.T.; Hui, K.K.W.; Li, H.; Chin, D.C.W.; Ju, S.; Heo, J.; Wong, M.S. Tree tilt monitoring in rural and urban landscapes of Hong Kong using smart sensing technology. *Trees For. People* **2020**, *2*, 100030. [\[CrossRef\]](#)
- Baker, C.J.; Bell, H.J. The aerodynamics of urban trees. *J. Wind. Eng. Ind. Aerodyn.* **1992**, *44*, 2655–2666. [\[CrossRef\]](#)
- Takahashi, K.; Aoike, K. GPR Measurements for Diagnosing Tree Trunk. In Proceedings of the 2018 17th International Conference on Ground Penetrating Radar, Rapperswil, Switzerland, 18–21 June 2018.
- James, K. A Study of Branch Dynamics on an Open-Grown Tree. *Arboric. Urban For.* **2014**, *40*, 125–134. [\[CrossRef\]](#)
- Sellier, D.; Fourcaud, T.; Lac, P. A finite element model for investigating effects of aerial architecture on tree oscillations. *Tree Physiol.* **2006**, *26*, 799–806. [\[CrossRef\]](#)
- Moore, J.R.; Maguire, D.A. Natural sway frequencies and damping ratios of trees: Concepts, review and synthesis of previous studies. *Trees* **2004**, *18*, 195–203. [\[CrossRef\]](#)
- Caponero, M.A.; Mongelli, M.; Imbimbo, M.; Modoni, G.; Polito, E.; Grande, E. Structural monitoring of the Ninfeo Ponari by fibre optic sensors, photogrammetry and laser scanning. *Archeol. Calc.* **2020**, *31*, 223–232. [\[CrossRef\]](#)
- Grande, E.; Imbimbo, M. A data-driven approach for damage detection: An application to the ASCE steel benchmark structure. *J. Civ. Struct. Health Monit.* **2012**, *2*, 73–85. [\[CrossRef\]](#)
- Grande, E.; Imbimbo, M.; Tomei, V. A Two-Stage Approach for the Design of Grid Shells. In Proceedings of the Structures and Architecture—Proceedings of the 3rd International Conference on Structures and Architecture, ICSA, Guimaraes, Portugal, 27–29 July 2016; pp. 551–557.
- Grande, E.; Imbimbo, M. A data fusion based approach for damage detection in linear systems. *Frat. Integrita Strutt.* **2014**, *8*, 325–333. [\[CrossRef\]](#)
- Grande, E.; Imbimbo, M. A multi-stage data-fusion procedure for damage detection of linear systems based on modal strain energy. *J. Civ. Struct. Health Monit.* **2014**, *4*, 107–118. [\[CrossRef\]](#)
- Grande, E.; Imbimbo, M. A multi-stage approach for damage detection in structural systems based on flexibility. *Mech. Syst. Signal Process* **2016**, *76–77*, 455–475. [\[CrossRef\]](#)
- Giachetti, A.; Zini, G.; Giambastiani, Y.; Bartoli, G. Field Measurements of Tree Dynamics with Accelerometers. *Forests* **2022**, *13*, 1243. [\[CrossRef\]](#)
- Moore, J.R.; Maguire, D.A. Simulating the dynamic behavior of Douglas-fir trees under applied loads by the finite element method. *Tree Physiol.* **2008**, *28*, 75–83. [\[CrossRef\]](#)

21. Hoag, D.L.; Fridley, R.B.; Hutchinson, J.R. Experimental measurement of internal and external damping properties of tree limbs. *Trans. ASAE* **1971**, *14*, 20–28. [[CrossRef](#)]
22. Solomon, O.M., Jr. *PSD Computations Using Welch's Method. [Power Spectral Density (PSD)]*; USDOE: Washington, DC, USA, 1991. [[CrossRef](#)]
23. The Mathworks, Inc. MATLAB, Version 9.0, 2016 MATLAB—MathWorks—MATLAB. Available online: www.mathworks.com/products/matlab2016 (accessed on 1 March 2023).
24. Lenci, S.; Consolini, L.; Clementi, F. On the experimental determination of dynamical properties of laminated glass. *Ann. Solid Struct. Mech.* **2015**, *7*, 27–43. [[CrossRef](#)]
25. Zhen, L.; Jiachen, L.; Huoxing, L.; Hongbo, Z.; Rongchao, X.; Filip, G. Stress Distribution in Direct Shear Loading and its Implication for Engineering Failure Analysis. *Int. J. Appl. Mech.* **2023**, *15*, 2350036. [[CrossRef](#)]
26. Laurin, G.V.; Francini, S.; Luti, T.; Chirici, G.; Pirotti, F.; Papale, D. Satellite open data to monitor forest damage caused by extreme climate-induced events: A case study of the Vaia storm in Northern Italy. *For. Int. J. For. Res.* **2020**, *94*, 407–416. [[CrossRef](#)]
27. Bolyn, C.; Lejeune, P.; Michez, A.; Latte, N. Mapping tree species proportions from satellite imagery using spectral–spatial deep learning. *Remote Sens. Environ.* **2022**, *280*, 113205. [[CrossRef](#)]

Disclaimer/Publisher's Note: The statements, opinions and data contained in all publications are solely those of the individual author(s) and contributor(s) and not of MDPI and/or the editor(s). MDPI and/or the editor(s) disclaim responsibility for any injury to people or property resulting from any ideas, methods, instructions or products referred to in the content.